A R C H I V E O F M E C H A N I C A L E N G I N E E R I N G

Volume 66 2019 Number 1

DOI: 10.24425/ame.2019.126368

Key words: small-sized beam, nonlocal theory, temperature-dependent properties, free lateral vibration

Alireza Babaei[1,2], Arash Rahmani[3], Isa Ahmadi[4]

Transverse vibration analysis of nonlocal beams with various slenderness ratios, undergoing thermal stress

In this paper, thermally-excited, lateral free vibration analysis of a small-sized Euler-Bernoulli beam is studied based on the nonlocal theory. Nonlocal effect is exerted into analysis utilizing differential constitutive model of Eringen. This model is suitable for design of sensors and actuators in dimensions of micron and submicron. Sudden temperature rise conducted through the thickness direction of the beam causes thermal stresses and makes thermo-mechanical properties to vary. This temperature field is supposed to be constant in the lateral direction. Temperatures of the top and bottom surfaces of the system are considered to be equal to each other. Governing equation of motion is derived using Hamilton's principle. Numerical analysis of the system is performed by Galerkin's approach. For verification of the present results, comparison between the obtained results and those of benchmark is reported. Numerical results demonstrate that dynamic behavior of small-sized system is been effected by temperature shift, nonlocal parameter, and slenderness ratio. As a result, taking the mentioned parameters into account leads to better and more reliable design in miniaturized-based industries.

1. Introduction

Through recent decades, micro and nano-electro-mechanical systems (MEMS, NEMS) technology has widely engrossed several researchers. Because of the advantages such as: cost-effectiveness, long life duration and high performance level,

✉ Alireza Babaei, e-mail: Alireza.Babaei@uky.edu

[1]Department of Mechanical Engineering, University of North Dakota, Grand Forks, North Dakota, USA.

[2]Department of Mechanical Engineering, University of Kentucky, Lexington, Kentucky, USA.

[3]Faculty of Mechanical Engineering, Urmia University of Technology, Urmia, Iran.

[4]Faculty of Mechanical Engineering, University of Zanjan, Zanjan, Iran.

it is worth to spend time and investigate these devices with in-depth consideration. MEMS/ NEMS can be generally defined as a technology including miniaturized electro-mechanical and mechanical elements which is accompanied with micro-fabrication techniques. The most noticeable applications of such technology are micro-sensors, micro-actuators and micro-electronics. Small-scaled beams are amongst the most applicable structures to model such systems. Moreover, several experiments have proved the essentiality of considering the size-dependency phenomena for analyzing such micro-system's mechanical behavior [1–4]. It is evident that theories based on the classical continuum do not consider size-dependent behavior; consequently, several researchers provided the scientific community with higher order continuum theories capturing the small effects thorough the analysis. Couple stress theory containing four material constants [5], micro-polar theory [6], nonlocal elasticity theory [7], strain gradient theory [8], modified couple stress theory with single material constant [9] and surface elasticity theory [10] are such non-classical theories capturing the size-dependencies of MEMS/NEMS models in the analysis.

Examples of researchers who have utilized the modified couple stress theory are: Roque et al. [11] conducted a research concerning bending analysis of a Timoshenko micro-beam using meshless approach with radial basis functions. Ghanbari et al. [12] studied vibration behavior of a small-scaled beam using assumed modes method. Askari et al. [13] reported dynamic, size-dependent analysis of MEMS elements under mechanical shock. Jung et al. [14] studied buckling and vibration behavior of micro-plates embedded in elastic medium. Free vibration analysis of a small-sized beam made up of functionally graded materials is presented by Babaei et al. [15]. Size-dependent vibration analysis of non-uniform, functionally graded small-scaled beam is reported by Shafiei et al. [16], they assumed Euler-Bernoulli and Timoshenko beam theories. Aghazadeh et al. [17] proposed a new functionally graded beam model with varying length scale parameter to investigate static and vibration analysis of small-sized electro-mechanical systems. Fathalilou et al. [18] have perused micro-inertia effect upon dynamic characteristics of a small-scaled beam.

Amongst the mentioned non-classical continuum theories, nonlocal theory is attractive to researchers: vibration analysis of a post-buckled piezoelectric small-sized beam is reported by Ansari et al. [19]. Eltaher et al. [20] presented a functionally graded nonlocal beam model to investigate the dynamic responses based on slenderness ratio ant the material gradation index. A similar research is carried out by Ebrahimi and Salari [21] which considers shear deformations and thermal effects in the analysis. Taking into account the thermal effects, vibration behavior of a functionally graded small-scaled beam is presented by Ebrahimi and Salari [22]. Babaei and Ahmadi [23] studied dynamic analysis of non-homogenous beams. They represented results based on a numerical approach. Babaei and Yang [24] carried out a research regarding rotation effects upon vibration analysis of rods. They used coupled-type field of displacements for the first time. Dynamic and vibration

analysis of micro-sensors based in the modified couple stress theory is reported by Babaei et al. [25]. They proposed the material length scale parameter as a variable one and investigated corresponding consequences on the response of the system. Azizi et al. [26] studied nonlinear vibration analysis of nano-beams embedded in elastic medium considering effects of surface stress effects. Safaei and Fattahi [27] carried out a research regarding vibrational behavior of single-layered Graphene sheets based on diverse nonlocal plate theories. Buckling analysis of carbon-nanotube reinforced beams with different boundary conditions is investigated by Fattahi and Safaei [28].

Capturing a realistic idea, temperature variations (especially in the shape of temperature rises) is an expectable phenomena. Usually, the mentioned temperature rises are induced to the system gradually. This temperature is mostly derived from the energy loss emitted from machinery working in the vicinity of the system. Hence it seems to be a proper assumption to take into account the thermal stresses besides to the small effects in the analysis. In the event of this notion, several scholars have considered the role played by heat conduction. Chakraborty et al. [29] studied the thermo-elastic behavior of a model made up of functionally graded material, and using the first-order shear deformation beam theory. Xiang and Yang [30] proposed a classic beam model to obtain free and forced vibration analysis of a laminated structure in which thermal stress effects are also captured. Based on the classic mechanics, thermo-dynamical analysis of a sandwich beam is reported by Pradhan and Murmu [31]. Vibrational analysis of micro-beam undergoing temperature conductions is accomplished by Nateghi and Salamat-talab [32], in this research material properties vary based on the rule of mixture. Mahi et al. [33] reported a similar research including material variations due to temperature besides to those induced by the grading characteristic. Eventually; Babaei et al. [34] presented a micro-beam model taking into account variations induced both by temperature and by material gradation, they obtained the formulas utilizing the modified couple stress and the Euler-Bernoulli beam theories. Safaei and Moradi-Dastjerdi [35] analyzed vibration behavior of thermo-elastic nano-plates reinforced by carbon nano-tubes.

Based on the review literature presented above and to the best of our knowledge, there are two researches in which nonlocal theory is adopted along with thermal stress effects upon vibration behavior of a small-sized system. Ebrahimi and Salari [21, 22] considered Timoshenko beam theory undergoing thermal stresses. In the current research, to achieve more accuracy of dynamic analysis of long beams, Euler-Bernoulli beam theory is adopted. Another difference includes the course of temperature difference. Ebrahimi and Salari have defined temperature shift as the difference of temperature between the top surface and the bottom one, so they have neglected the temperature difference between the system and the environment. However, for considering the heat-energy lost from machinery or other appliances, we have presented another temperature-rise feature. This rise is the temperature difference between the beam surfaces and the environment. In other words, purpose

of this study includes the effects of thermal stresses derived from temperature difference between the structure itself and the surrounding area.

In this paper, based on the Eringen's nonlocal constitutive equations; a simply-supported thermally-stressed Euler-Bernoulli beam model is presented for free lateral vibration analysis. Initial temperature rise along the thickness direction of the beam causes thermal stresses. Throughout the cross section plane, temperature field is supposed to be in steady state. Besides, different values for slenderness ratio (ratio of the beam length to the beam thickness) are considered in this analysis. In order to derive the governing equation of motion, Hamilton's principle is taken, for solution procedure Galerkin's method is adopted.

2. Theory and preliminaries

Based on the Eringen [7]; in an elastic medium, stress field at a random point x is a function of both the strain field corresponding to that point (hyperelastic case) and all other strain fields of the configuration. General from of nonlocal characteristic equation is shown in Eq. (1) [7]:

$$\left[1 - (e_0 a)^2 \nabla^2\right] t_{kl} = \lambda \varepsilon_{rr} \delta_{kl} + \mu \varepsilon_{kl} \,. \tag{1}$$

In Eq. (1), t_{kl} is nonlocal stress tensor, ε_{kl} and ε_{rr} represent strain tensor, δ_{kl} is the Kronecker delta function, λ and μ are Lame's constants. $(e_0 a)^2$ is named as nonlocal parameter; where, e_0 is occasionally specific for each material and a represents the internal characteristic length. Nonlocal constitutive relation can be found in the following form [7]:

$$\sigma_{xx} - (e_0 a)^2 \frac{\partial^2 \sigma_{xx}}{\partial x^2} = E \varepsilon_{xx} \,. \tag{2}$$

In the above equations, σ_{xx} and ε_{xx} represent axial normal stress and axial strain. σ_{xz} is shear stress, and γ_{xz} is shear strain. E and G are elasticity modulus and modulus of rigidity which are constrained to each other ($G = E/2(1 + \nu)$), ν is Poison's ratio). By putting the nonlocal parameter equal to zero, constitutive relation of local theory is achievable.

3. Mathematical modeling

3.1. Kinematic relations

According to the Euler-Bernoulli beam theory before and after deformation, plane sections perpendicular to the axis of the beam remain perpendicular and rotate such that no distortion is resulted. As a result, axial and lateral displacements

(u_x, u_z) of any point of the beam are as follows [34]:

$$u_x(x,z,t) = -z\frac{\partial w}{\partial x}, \tag{3a}$$

$$u_y(x,z,t) = 0, \tag{3b}$$

$$u_z(x,z,t) = w(x,t), \tag{3c}$$

where, w denotes lateral displacement of any point on the mid plane and t represents time. The only nonzero strain is the bending strain:

$$\varepsilon_{xx} = -z\frac{\partial^2 w}{\partial x^2}. \tag{4}$$

3.2. Thermal induction

A simply-supported beam of length L, thickness h and width b is considered and shown in Fig. 1.

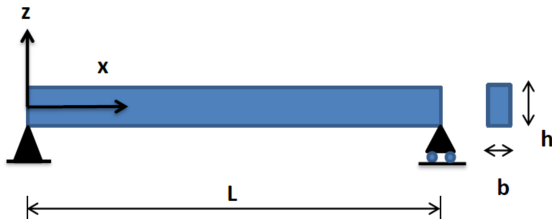

Fig. 1. Geometry of a nonlocal simply-supported beam

The mentioned beam is located in a temperature-varying environment without any heat generation. Furthermore, heat transfer is considered only through the lateral direction. Hence; following steady-state, one dimensional heat conduction equation fits the case [34]:

$$\frac{\mathrm{d}}{\mathrm{d}z}\left[k(z)\frac{\mathrm{d}T}{\mathrm{d}z}\right] = 0. \tag{5}$$

In Eq. (5), $k(z)$ is thermal conductivity which is varying through the thickness direction of the beam. However; equal temperatures for the upper and lower surfaces will be considered, so there is not necessity to elaborate variation of thermal conduction coefficient. By applying boundary conditions ($T(z = h/2) = T_t$, $T(z = -h/2) = T_b$), unique solution of Eq. (6) takes the following form [34]:

$$T(z) = T_b + \frac{T_t - T_b}{\displaystyle\int_{-h/2}^{h/2}\frac{1}{k(z)}\,\mathrm{d}z}\int_{-h/2}^{z}\frac{1}{k(z)}\,\mathrm{d}z. \tag{6}$$

Thermal expansion coefficient (α) and modulus of elasticity (E) are supposed to be temperature-dependent. Such properties are obtainable based on the following relation [34]:

$$P = P_0 \left(P_{-1} T^{-1} + 1 + P_1 T + P_2 T^2 + P_3 T^3 \right). \tag{7}$$

In Eq. (7) P_{-1}, P_0, P_1, P_2 and P_3 are constant temperature coefficients. Temperature difference between any random point on the perpendicular section and the environment is as follows:

$$\Delta T = T_s - T_0 \,. \tag{8}$$

Temperature of the environment is supposed to be a fixed one ($T_0 = 20^\circ$C). It is also good to note that temperature of the top and bottom surfaces are equal to the environment temperature at first. With a sudden rise in the temperature of the beam's upper or lower surface, thermal stress is expected. Based on Babaei [34], the mentioned thermal stress term is represented by Eq. (9):

$$\sigma_{xx}{}^{T} = -E(T)\alpha(T)\nabla T. \tag{9}$$

As mentioned above, modulus of elasticity and thermal expansion coefficient are temperature-dependent. It means for each temperature induced to the surfaces of the beam, thermo-mechanical properties take a specific value. In Figs. 2 and 3, influence of temperature on the modulus of elasticity and thermal expansion coefficient are shown. Other properties' changes are not of importance since they do not appear in the governing equation of motion. Based on Fig. 2, modulus of elasticity decreases by increasing in the value of temperature; while, Fig. 3 demonstrates linear increment for values of thermal expansion coefficient when temperature arises. It is good to note that the two mentioned figures, are plotted using Eq. (7) and Table 1.

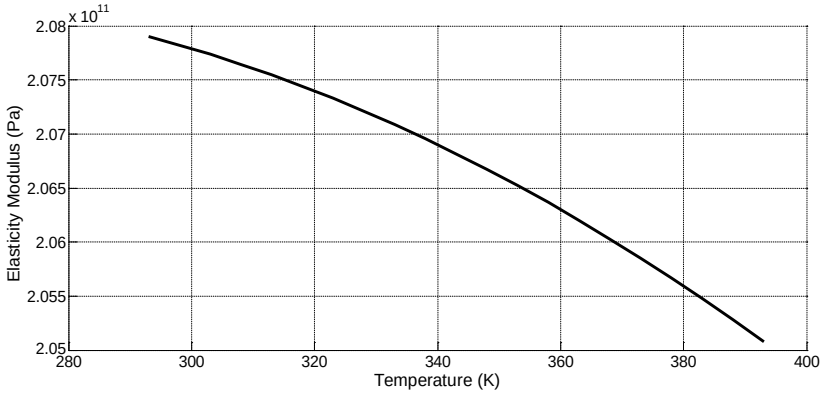

Fig. 2. Variation of elasticity modulus with temperature

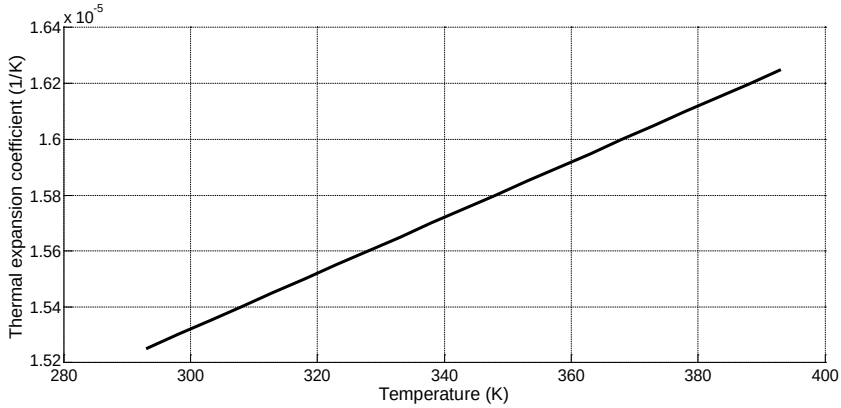

Fig. 3. Variation of thermal expansion coefficient with temperature

Table 1.
Temperature-dependent coefficients of stainless steel (SUS3O4) at $T = 0$ K (Young's modulus E (Pa), coefficient of thermal expansion α (1 K^{-1})) [34]

Property	P_{-1}	P_0	P_1	P_2	P_3
E	0	201.04×10^9	3.079×10^{-4}	-6.534×10^{-7}	0
α	0	12.33×10^{-6}	8.086×10^{-4}	0	0

3.3. Governing equation of motion

In order to obtain the equation of motion, Hamiltoon's principle is used. Based on this variational approach, variation of the Lagrangian of the system ($\mathcal{L}$) is equal to zero over a time interval [34].

$$\delta \left[\int_{t_1}^{t_2} \mathcal{L} \, \mathrm{d}t \right] = 0. \tag{10}$$

Lagrangian means the difference between kinetic (U_K) and potential energies (U) of the system [15]:

$$\mathcal{L} = U_K - U. \tag{11}$$

Kinetic energy U_K of Euler-Bernoulli beam can be expressed in the following form [15]:

$$U_K = \frac{1}{2} \int_V \rho \left(\frac{\partial w}{\partial t} \right)^2 \mathrm{d}V, \tag{12a}$$

where ρ represents density and integration's domain for the energy terms is over volume.

Potential energy of this system includes the energy resulting from toughness (U_S) which is mostly named as strain energy and the energy resulting from heat conduction (U_T) [34]:

$$U = U_T + U_S, \tag{12b}$$

$$U_S = \int_V \sigma_{xx}\,\varepsilon_{xx}\,\mathrm{d}V, \tag{12c}$$

$$U_T = \frac{1}{2}\int_V {\sigma_{xx}}^T \left(\frac{\partial w}{\partial x}\right)^2 \mathrm{d}V. \tag{12d}$$

The first variation of kinetic energy is obtained as:

$$\delta U_K = \int_V \rho \frac{\partial w}{\partial t}\,\frac{\partial}{\partial t}\delta w\,\mathrm{d}V. \tag{13}$$

The first variations of the potential energies are given as:

$$\delta U_T = \int_V {\sigma_{xx}}^T \frac{\partial w}{\partial x}\,\frac{\partial}{\partial x}\delta w\,\mathrm{d}V, \tag{14}$$

$$\delta U_S = \int_V \sigma_{xx}\delta\varepsilon_{xx}\,\mathrm{d}V. \tag{15}$$

Using Eq. (9) and Eq. (14) takes the following form:

$$\delta U_T = -\int_0^L E(T)\alpha(T)A\Delta T\frac{\partial w}{\partial x}\,\frac{\partial}{\partial x}\delta w\,\mathrm{d}x. \tag{16}$$

By substituting Eq. (4) into Eq. (15), Eq. (17) is obtained:

$$\delta U_S = \int_V -z\sigma_{xx}\frac{\partial^2}{\partial x^2}\delta w\,\mathrm{d}V. \tag{17}$$

By introducing bending moment as the second stress resultant in Eq. (18), Eq. (17) can be rewritten as Eq. (19):

$$M = \int_A z\sigma_{xx}\,\mathrm{d}A, \tag{18}$$

$$\delta U_s = -\int_0^L M\frac{\partial^2}{\partial x^2}\delta w\,\mathrm{d}x. \tag{19}$$

Eq. (13) can be converted to integration over the area of the cross section:

$$\delta U_K = \int_0^L \rho A \frac{\partial w}{\partial t} \frac{\partial}{\partial t} \delta w \, \mathrm{d}x. \tag{20}$$

Substituting Eqs. (16), (19) and (20) into the Eq. (10) leads to the following equation:

$$\int_{t_1}^{t_2} \int_0^L \left\{ \rho A \frac{\partial w}{\partial t} \frac{\partial}{\partial t} \delta w + M \frac{\partial^2}{\partial x^2} \delta w + S \frac{\partial w}{\partial x} \frac{\partial}{\partial x} \delta w \right\} \mathrm{d}x \, \mathrm{d}t = 0. \tag{21}$$

In Eq. (21), $S = E(T)\alpha(T)A\Delta T$. By integration by parts on Eq. (21), Eq. (22) is concluded:

$$\int_{t_1}^{t_2} \int_0^L \left(\frac{\partial^2 M}{\partial x^2} - S \frac{\partial^2 w}{\partial x^2} - \rho A \frac{\partial^2 w}{\partial t^2} \right) \delta w \, \mathrm{d}x \, \mathrm{d}t + \int_{t_1}^{t_2} \left\{ \frac{\partial M}{\partial x} \delta w \Big|_0^L - S \frac{\partial w}{\partial x} \delta w \Big|_0^L - M \frac{\partial \delta w}{\partial x} \Big|_0^L \right\} \mathrm{d}t = 0. \tag{22}$$

As a result, the equation of motion and the boundary conditions of the simply-supported nonlocal beam are obtained:

$$\rho A \frac{\partial^2 w}{\partial t^2} - \frac{\partial^2 M}{\partial x^2} + S \frac{\partial^2 w}{\partial x^2} = 0, \tag{23}$$

$$w|_{x=0,\,L} = 0, \qquad \frac{\partial^2 w}{\partial x^2}\bigg|_{x=0,\,L} = 0. \tag{24}$$

Using Eqs. (2), (4) and (18); moment-strain relation of the nonlocal Euler-Bernoulli beam is achieved:

$$M - (e_0 a)^2 \frac{\partial^2 M}{\partial x^2} = -EI \frac{\partial^2 w}{\partial x^2}, \tag{25}$$

where I is second moment of inertia of the beam's cross section.

By substituting second derivative of the nonlocal bending moment from Eq. (23) into Eq. (25), an explicit relation for the second stress resultant (M) is obtainable:

$$M = (e_0 a)^2 \left[\rho A \frac{\partial^2 w}{\partial t^2} + S \frac{\partial^2 w}{\partial x^2} \right] - EI \frac{\partial^2 w}{\partial x^2}. \tag{26}$$

Finally, the explicit nonlocal governing equation of motion in terms of lateral displacement can be derived by substituting second derivative of Eq. (26) into

Eq. (23) as follows:

$$\rho A\frac{\partial^2 w}{\partial t^2} - (e_0 a)^2\left[\rho A\frac{\partial^4 w}{\partial x^2 \partial t^2} + S\frac{\partial^4 w}{\partial x^4}\right] + EI\frac{\partial^4 w}{\partial x^4} + S\frac{\partial^2 w}{\partial x^2} = 0. \tag{27}$$

Ignoring temperature difference ($\Delta T = 0$) in Eq. (27) leads to the governing equation of nonlocal Euler-Bernoulli beam.

4. Solution procedure

For the case of free vibrations; since there is no trace of any external forces or viscous damping, lateral displacement can be expressed as in the following shape:

$$w(x,t) = y(x)e^{r\omega t}, \tag{28}$$

in which ω denotes the natural angular frequency, $y(x)$ is the amplitude of vibrations and $r = \sqrt{-1}$. Using Eq. (28), Eq. (27) reaches the following form:

$$\left(EI - (e_0 a)^2 S\right)\frac{\mathrm{d}^4 y}{\mathrm{d}x^4} + \left(S + (e_0 a)^2 \rho A\omega^2\right)\frac{\mathrm{d}^2 y}{\mathrm{d}x^2} - \rho A\omega^2 y = 0. \tag{29}$$

Dimensionless variables are defined as follows:

$$\begin{gathered} X = \frac{x}{L}, \qquad Y = \frac{y}{L}, \qquad \eta = \frac{e_0 a}{L}, \\ \widehat{\omega} = \omega L^2\sqrt{\frac{\rho A}{EI - (e_0 a)^2 S}}, \quad q = \frac{SL^2}{EI - (e_0 a)^2 S}. \end{gathered} \tag{30}$$

As such, the equation of motion (Eq. (29)) is simplified into the following dimensionless equation

$$\frac{\mathrm{d}^4 Y}{\mathrm{d}X^4} + \left(q + \eta^2\widehat{\omega}^2\right)\frac{\mathrm{d}^2 Y}{\mathrm{d}X^2} - \widehat{\omega}^2 Y = 0. \tag{31}$$

In this section, Galerkin's method is adopted. Based on Babaei et al. [34] this approximate method discretizes the continuous system into a discrete system utilizing expansion series.

$$Y(X) = \sum_{i=1}^{n} b_i \varphi_i(X). \tag{32}$$

In Eq. (32), mode shape functions are considered as a linear combination of trial functions ($\varphi_i(X)$) and undetermined coefficients (b_i). Trial functions are a complete set of independent functions. This procedure is equivalent to applying the method of variation of parameters to a function space. Constraints should be applied on the function space in order to characterize the space with a set of trial

functions. Such functions also play the role of test or weighting functions. It is essential to choose proper trial functions satisfying natural and geometric boundary conditions. For a simply-supported (pinned-pinned) beam, following sinusoidal functions are adopted (however other functions satisfying the boundary conditions can also be used):

$$\varphi_i(X) = \sin(i\pi X), \quad i = 1, 2, 3, \ldots \tag{33}$$

Substitution Eq. (32) into Eq. (31) leads to the following equation

$$\sum_{i=1}^{n} b_i \frac{\mathrm{d}^4\varphi_i(X)}{\mathrm{d}X^4} + \left(q + \eta^2\widehat{\omega}^2\right) \sum_{i=1}^{n} b_i \frac{\mathrm{d}^2\varphi_i(X)}{\mathrm{d}X^2} - \widehat{\omega}^2 \sum_{i=1}^{n} b_i\varphi_i(X) = 0. \tag{34}$$

In order to use orthogonality of trial functions, Eq. (34) is to be multiplied by the weight functions $\varphi_j(X)$. Then, integration operation over the interval of the system leads the Galerkin procedure to the following equation:

$$\sum_{i=1}^{n} \int_0^1 b_i \frac{\mathrm{d}^4\varphi_i(X)}{\mathrm{d}X^4}\varphi_j(X)\,\mathrm{d}X + \left(q + \eta^2\widehat{\omega}_n^2\right) \sum_{i=1}^{n} \int_0^1 b_i \frac{\mathrm{d}^2\varphi_i(X)}{\mathrm{d}X^2}\varphi_j(X)\,\mathrm{d}X$$
$$- \widehat{\omega}^2 \sum_{i=1}^{n} b_i\varphi_i(X)\varphi_j(X)\,\mathrm{d}X = 0, \qquad j = 1, 2, 3, \ldots \tag{35}$$

After some mathematical manipulations, Eq. (35) reaches a set of linear algebraic homogenous equations in the unknowns b_i which can be numerically solved and dimensionless frequencies ($\widehat{\omega}$) can be obtained.

5. Results and discussion

In this section, numerical results concerning the vibration behavior of a simply-supported nonlocal Euler-Bernoulli beam are presented. Thermo-mechanical properties of the beam are shown in Table 1. It is a major note that modulus of elasticity (E), and thermal expansion coefficient (α) are varying based on the temperature shifts. Such variations in the value of E and α explicitly affect the frequency due to the additional term caused by thermal stresses. Beams length is $L = 10000$ nm. Thickness is variable and different values for the ratio of length to the thickness (slenderness ratio) are considered. Numerical results are obtained using the dimensionless frequency relation $\left(\widehat{\omega} = \omega L^2\sqrt{(\rho A/EI - (e_0a)^2S)}\right)$, in which $I = bh^3/12$ is the second moment of inertia and $A = bh$ is the area of the cross section. In order to check the validity of the present model, present results are compared with those of Reddy [36] and Eltaher et al. [20]. This verification given in Table 2 approves the accuracy and validity of the present results. As it is evident in the formula

Table 2.

Comparison of dimensionless frequencies of first three vibration modes ($L/h = 100$)

$\widehat{\omega}_n$	η^2	0	1	2	3	4
$n = 1$	Present	9.8696	9.4159	9.0195	8.6693	8.3569
	Eltaher et al. (2012)	9.8700	9.4162	9.0197	8.6695	8.3571
	Reddy (2007)	9.8696	9.4159	9.0195	8.6693	8.3569
$n = 2$	Present	39.4784	33.4277	29.5111	26.7115	24.5823
	Eltaher et al. (2012)	39.4849	33.4301	29.5117	26.7111	24.5814
$n = 3$	Present	88.8264	64.6414	53.3078	46.4000	41.6285
	Eltaher et al. (2012)	88.8594	64.6429	53.3024	46.3922	41.6199

presented above, existence of S demonstrates that temperature should play a direct role in the dimensionless frequency.

Table 3 shows dimensionless fundamental frequencies for a system undergoing temperature shifts. Results are reported for different values of nonlocal parameter ($\eta^2 = 1, 2, 3, 4$) and for classical case ($\eta^2 = 0$). Starting from initial surface temperature ($T = 20^\circ$C), an increment of 2.5°C is exerted and slenderness ration is supposed to be a fixed one ($L/h = 50$). Tables 4 and 5 give the similar results for dimensionless second and third frequencies. The only difference refers to the fact that temperature increment takes greater values and this is mainly because of covering more comprehensive frequency domain. Based on Tables 3, 4 and 5; dimensionless frequency of both classical and nonlocal beam, decreases with temperature rises. Moreover, capturing greater nonlocal parameter ends up in further decrement in the frequency. For the same thermally-stressed system, dimensionless fundamental frequency's dependency on slenderness ratios ($L/h = 10, 25, 50, 75, 100$) are shown in Table 6. Results are calculated for both classical and nonlocal beams. Tables 7 and 8 show the same results for dimensionless second and third

Table 3.

Variation of dimensionless fundamental frequencies for different temperatures (based on classical ($\eta = 0$) and nonlocal theories ($\eta \neq 0$), $L/h = 50$)

$\widehat{\omega}_1$	$\eta^2 = 0$	$\eta^2 = 1$	$\eta^2 = 2$	$\eta^2 = 3$	$\eta^2 = 4$
$T_s = 20$	9.8696	9.4159	9.0195	8.6693	8.3569
$T = 22.5$	9.3870	8.9510	8.5698	8.2327	7.9319
$T = 25$	8.8762	8.4488	8.0739	7.7412	7.4429
$T = 27.5$	8.3318	7.9019	7.5213	7.1800	6.8705
$T = 30$	7.7470	7.2996	6.8965	6.5273	6.1839
$T = 32.5$	7.1116	6.6264	6.1755	5.7466	5.3286
$T = 35$	6.4108	5.8570	5.3165	4.7683	4.1865
$T = 37.5$	5.6199	4.9462	4.2326	3.4153	2.3393
$T = 40$	4.6938	3.7921	2.6554	0	0

Table 4.
Variation of dimensionless second frequencies for different temperatures (based on classical ($\eta = 0$) and nonlocal theories ($\eta \neq 0$), $L/h = 50$)

$\widehat{\omega}_2$	$\eta^2 = 0$	$\eta^2 = 1$	$\eta^2 = 2$	$\eta^2 = 3$	$\eta^2 = 4$
$T = 20$	39.4784	33.4277	29.5111	26.7115	24.5823
$T = 25$	38.5234	32.6033	28.7689	26.0261	23.9385
$T = 30$	37.5363	31.7167	27.9369	25.2240	23.1503
$T = 35$	36.5144	30.7595	26.9968	24.2712	22.1615
$T = 40$	35.4547	29.7215	25.9239	23.1182	20.8798
$T = 45$	34.3538	28.5900	24.6849	21.6885	19.1412
$T = 50$	33.2076	27.3489	23.2322	19.8560	16.6104
$T = 55$	32.0111	25.9774	21.4946	17.3868	12.3876
$T = 60$	30.7585	24.4473	19.3573	13.7481	0

Table 5.
Variation of dimensionless third frequencies for different temperatures (based on classical ($\eta = 0$) and nonlocal theories ($\eta \neq 0$), $L/h = 50$)

$\widehat{\omega}_3$	$\eta^2 = 0$	$\eta^2 = 1$	$\eta^2 = 2$	$\eta^2 = 3$	$\eta^2 = 4$
$T = 20$	88.8264	64.6414	53.3078	46.4000	41.6285
$T = 25$	87.8779	63.9378	52.7162	45.8746	41.1475
$T = 30$	86.9114	63.1923	52.0632	45.2697	40.5686
$T = 35$	85.9263	62.4009	51.3389	44.5658	39.8586
$T = 40$	84.9220	61.5592	50.5307	43.7359	38.9666
$T = 45$	83.8977	60.6620	49.6227	42.7425	37.8116
$T = 50$	82.8527	59.7034	48.5949	41.5310	36.2546
$T = 55$	81.7863	58.6766	47.4211	40.0187	34.0341
$T = 60$	80.6976	57.5735	46.0667	38.0732	30.5825
$T = 65$	79.5856	56.3849	44.4844	35.4654	24.2995
$T = 70$	78.4494	55.0996	42.6079	31.7516	0

frequencies. It is inferable that by increasing the length of the beam in comparison to the thickness, frequencies get smaller. As a result, temperature rises and slenderness ratio's increment, reinforce each other and affect the frequencies in similar way. Another finding is the fact that, frequencies can be ignored for specific nonlocal parameter with initial temperature rise and specific slenderness ratio. Table 3 shows this point when temperature is $T = 40°\text{C}$ and $\eta^2 = 3, 4$. This means that the first frequency of the system is zero and there is no vibration when the mentioned values of temperature and nonlocal parameter are considered. A similar procedure happens for second and third frequencies with higher temperatures and only when nonlocal parameter is equal to 4. It can be concluded that the state of zero-frequency

Table 6.
Variation of dimensionless fundamental frequencies with different values of slenderness ratio and temperature shifts (based on classical ($\eta = 0$) and nonlocal theories ($\eta = 2$))

$\widehat{\omega}_1$	η^2	$L/h = 10$	$L/h = 25$	$L/h = 50$	$L/h = 75$	$L/h = 100$
$\Delta T = 0$	0	9.8696	9.8696	9.8696	9.8696	9.8696
	2	9.0195	9.0195	9.0195	9.0195	9.0195
$\Delta T = 2$	0	9.8545	9.7750	9.4857	8.9827	8.2270
	2	9.0057	8.9327	8.6631	8.1791	7.4118
$\Delta T = 4$	0	9.8394	9.6792	9.0842	7.9947	6.1533
	2	8.9918	8.8442	8.2784	7.1653	4.9797
$\Delta T = 6$	0	9.8242	9.5822	8.6628	6.8620	2.8193
	2	8.9779	8.7537	7.8604	5.8782	0

Table 7.
Variation of dimensionless second frequencies with different values of slenderness ratio and temperature shifts (based on classical ($\eta = 0$) and nonlocal theories ($\eta = 2$))

$\widehat{\omega}_2$	η^2	$L/h = 10$	$L/h = 25$	$L/h = 50$	$L/h = 75$	$L/h = 100$
$\Delta T = 0$	0	39.4784	39.4784	39.4784	39.4784	39.4784
	2	29.5111	29.5111	29.5111	29.5111	29.5111
$\Delta T = 5$	0	39.4407	39.2418	38.5234	37.2953	35.5046
	2	29.4828	29.3326	28.7689	27.7229	25.9770
$\Delta T = 10$	0	39.4026	39.0020	37.5363	34.9572	30.9880
	2	29.4542	29.1480	27.9369	25.3810	19.7783
$\Delta T = 15$	0	39.3641	38.7587	36.5144	32.4306	25.6430
	2	29.4253	28.9571	26.9968	22.1332	0

Table 8.
Variation of dimensionless third frequencies with different values of slenderness ratio and temperature shifts (based on classical ($\eta = 0$) and nonlocal theories ($\eta = 2$))

$\widehat{\omega}_3$	η^2	$L/h = 10$	$L/h = 25$	$L/h = 50$	$L/h = 75$	$L/h = 100$
$\Delta T = 0$	0	88.8264	88.8264	88.8264	88.8264	88.8264
	2	53.3078	53.3078	53.3078	53.3078	53.3078
$\Delta T = 5$	0	88.7887	88.5903	87.8779	86.6777	84.9689
	2	53.2852	53.1648	52.7162	51.8970	50.5701
$\Delta T = 10$	0	88.7506	88.3516	86.9114	84.4566	80.8949
	2	53.2622	53.0174	52.0632	50.1294	46.3252
$\Delta T = 15$	0	88.7123	88.1104	85.9263	82.1574	76.5698
	2	53.2390	52.8654	51.3389	47.8452	38.7104
$\Delta T = 20$	0	88.6736	87.8666	84.9220	79.7731	71.9484
	2	53.2155	52.7088	50.5307	44.7673	18.1504

is reachable for small values of nonlocal parameter, if larger temperature shifts are exerted to the system.

Fig. 4 depicts variations of the fundamental dimensionless frequencies with temperature. It can be understood that after a critical temperature ($T = 60^{\circ}$C); nonlocal parameter turns out to be more severe in affecting the frequencies, since steep variations take place in the mentioned temperature domain. Figs 5 and 6 demonstrate the decrement in the second and the third frequencies by temperature increment. There are three other points caught from these figures: by taking greater nonlocal parameters, smaller frequencies should be expected. At an initial temperature, two frequencies get closer to each other if the corresponding nonlocal parameters are big values; in other words, as the nonlocal parameter gets greater the corresponding frequency gets closer to the frequency derived from the previous nonlocal parameter. Besides, Steep frequency variations in the second and third vibration modes take place at $T = 55^{\circ}$C, and $T = 65^{\circ}$C. Fig. 7 shows the influence

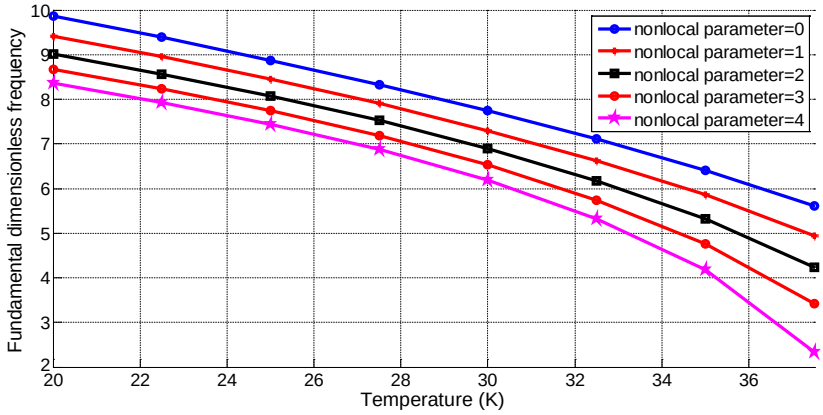

Fig. 4. Variations of fundamental dimensionless frequency with temperature

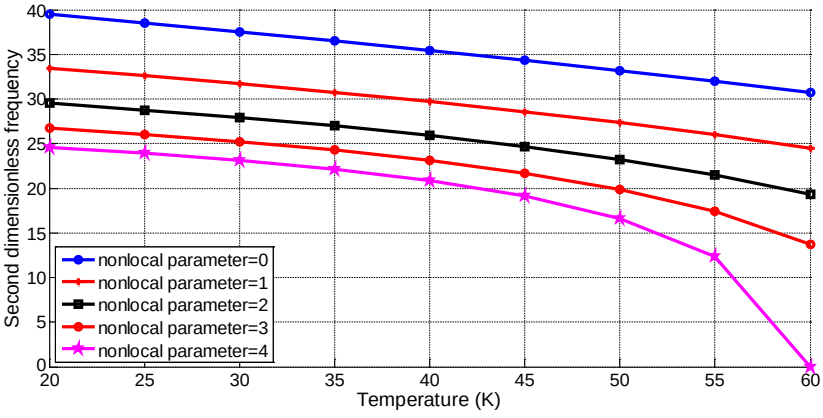

Fig. 5. Variations of second dimensionless frequency with temperature

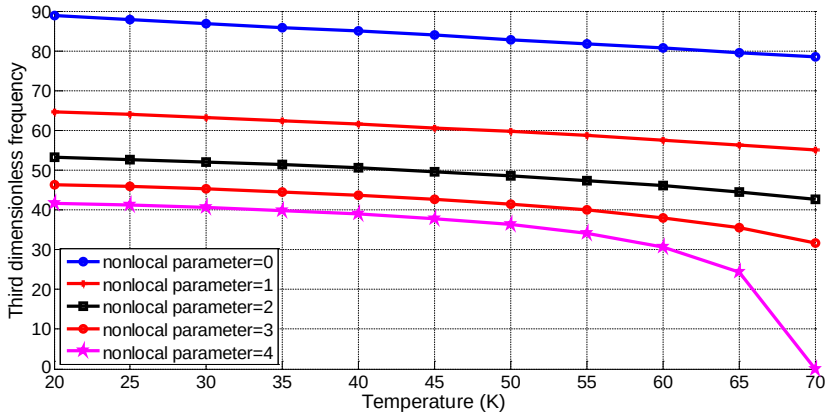

Fig. 6. Variations of third dimensionless frequency with temperature

of slenderness ratio upon fundamental dimensionless frequencies of the system bearing temperature rises. The longer and thinner beam ends up in smaller vibration frequencies. The other deduced point is the significant effect of the sudden temperature rises exerted to the upper and lower surfaces of the beam accompanied by the slenderness ratio effects. This figure demonstrates more impressive consequences caused by slenderness ratio if greater thermal energies are induced to the system. In other words, temperature rise complements and intensifies the effects of the slenderness ratio and vice versa. Moreover, Fig. 7b proves the effect of nonlocal parameter besides to the temperature and slenderness ratio effects. For the first vibration mode, slenderness ratio with the value of 50 ($L/h = 50$) is the changing point. As far as ratio of beam length to beam thickness is smaller than 50, frequency of the system is around a fixed value. However; for values greater than

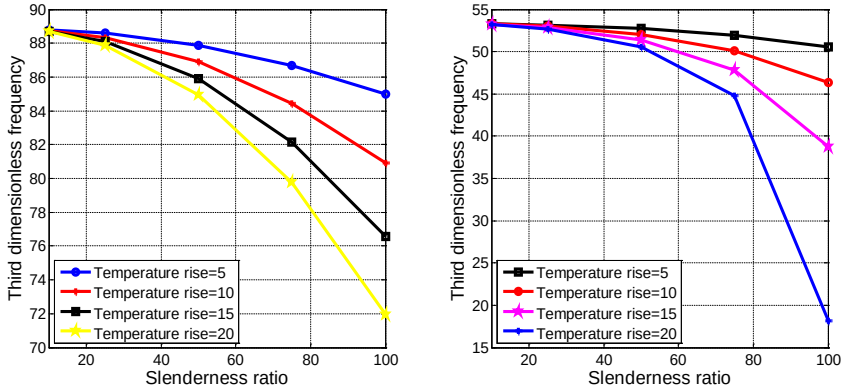

Fig. 7. Variations of fundamental dimensionless frequency with slenderness ratio: a) $\eta = 0$, b) $\eta = 2$

50 ($L/h > 50$) significant shifts in the frequency are observed. Figs. 8 and 9 depict the frequency shifts of the second and third modes of vibration showing that in the existence of the nonlocal parameter, intense decrement in frequency is expectable. There is changing point in the frequency value of each mode. By Fig. 8b; for values $L/h > 50$ accompanied by temperature rises over 15°C, frequency starts to decrease sharply and reaches zero when $L/h = 100$. Based on Fig. 9b; for the third mode, the steep decrement in frequency starts at $L/h > 50$ and temperature rises greater than 20°C. It shows that for higher vibration modes, greater temperature rises cause the frequency to drop significantly. Finally based on the tables and figures, it is evident that by considering the nonlocal effects, frequency estimations are less than those calculated based on the classical theory. From a mathematical

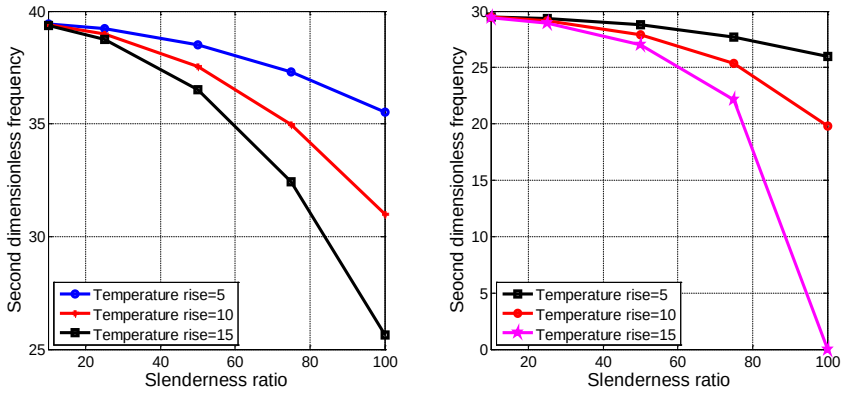

(a) (b)

Fig. 8. Variations of second dimensionless frequency with slenderness ratio: a) $\eta = 0$, b) $\eta = 2$

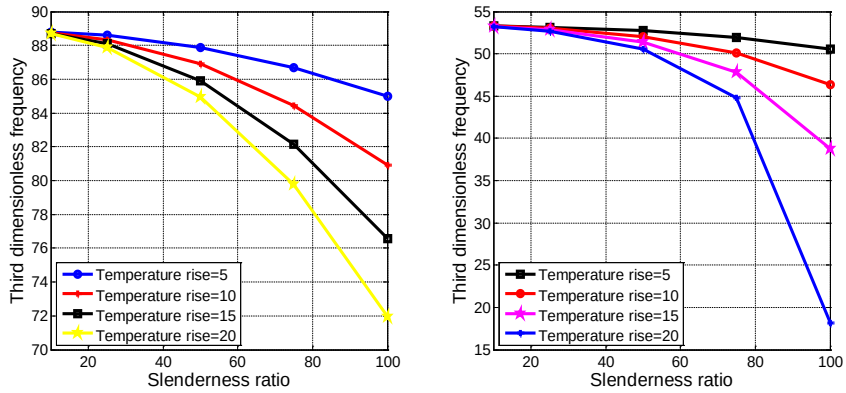

(a) (b)

Fig. 9. Variations of third dimensionless frequency with slenderness ratio: a) $\eta = 0$, b) $\eta = 2$

point of view, this is because a positive term is being added to the coefficient of square of frequency. Physically, it can be explained since using nonlocal theory, the stress at any point is a function of strain at all points of the configuration. Moreover, by comparison of the results of this paper and those reported by Babaei et al. [34], it can be concluded that different non-classical theories estimate the frequencies close to each other. However, this slight shifts can be important through the design procedure.

6. Conclusions

In this paper, free lateral vibration analysis of a small-scaled Euler-Bernoulli beam model undergoing thermal stresses is presented. To capture the size-dependencies, nonlocal effect is inserted according to the Eringen's nonlocal theory. The governing equation of motion is derived based on the principle of virtual work and the solution procedure is established based on the Galerkin's approximate method. According to the type of the boundary conditions (pinned-pinned), sinusoidal trial functions are chosen as mode shape functions. Results prove that frequencies obtained based on the nonlocal theory are smaller than those obtained from the classical theory and those reported by Babaei [34], and the difference turns out to be more significant in the second and third modes of vibration. Moreover, it is also feasible to reach the desired frequency domain by manipulating slenderness ratio. Temperature effect in the form of thermal stress is another factor affecting the frequencies of the model remarkably. Finally, considering proper surface temperatures and appropriate slenderness ratio leads to a desirable and expectable behavior of small-sized systems.

Manuscript received by Editorial Board, July 13, 2018;
final version, October 29, 2018.

References

[1] R.A. Toupin. Elastic materials with couple-stresses. *Archive for Rational Mechanics and Analysis*, 11(1):385–414, 1962. doi: 10.1007/BF00253945.

[2] R. Mindlin and H. Tiersten. Effects of couple-stresses in linear elasticity. *Archive for Rational Mechanics and Analysis*, 11(1):415–448, 1962. doi: 10.1007/BF00253946

[3] A. Ghanbari and A. Babaei. The new boundary condition effect on the free vibration analysis of micro-beams based on the modified couple stress theory. *International Research Journal of Applied and Basic Sciences*, 9(3):274–9, 2015.

[4] N. Fleck and J. Hutchinson. A phenomenological theory for strain gradient effects in plasticity. *Journal of the Mechanics and Physics of Solids*, 41(12):1825–1857,1993. doi: 10.1016/0022-5096(93)90072-N.

[5] R. Mindlin. Influence of couple-stresses on stress concentrations. *Experimental Mechanics*, 3(1):1–7, 1963. doi: 10.1007/BF02327219.

[6] A.C. Eringen. Theory of micropolar plates. *Zeitschrift für Angewandte Mathematik und Physik (ZAMP)*, 18(1):12–30, 1967. doi: 10.1007/BF01593891.

[7] A.C. Eringen. Nonlocal polar elastic continua. *International Journal of Engineering Science*, 10(1):1–16, 1972. doi: 10.1016/0020-7225(72)90070-5.

[8] E.C. Aifantis. Strain gradient interpretation of size effects. *International Journal of Fracture*, 95(1):299–314, 1999. doi: 10.1023/A:1018625006804.

[9] F. Yang, A.C.M. Chong, D.C.C. Lam, and P. Tong. Couple stress based strain gradient theory for elasticity. *International Journal of Solids and Structures*, 39(10):2731–2743, 2002. doi: 10.1016/S0020-7683(02)00152-X.

[10] M. Gurtin, J. Weissmüller, and F. Larché. A general theory of curved deformable interfaces in solids at equilibrium. *Philosophical Magazine A*, 78(5):1093–1109, 1998. doi: 10.1080/01418619808239977.

[11] C.M.C Roque, D.S. Fidalgo, A.J.M. Ferreira, and J.N. Reddy. A study of a microstructure-dependent composite laminated Timoshenko beam using a modified couple stress theory and a meshless method. *Composite Structures*, 96:532–537, 2013. doi: 10.1016/j.compstruct.2012.09.011.

[12] A. Ghanbari, A. Babaei, and F. Vakili-Tahami. Free vibration analysis of micro beams based on the modified couple stress theory, using approximate methods. *International Journal of Engineering and Technology Sciences*, 3(2):136–143, 2015.

[13] A.R. Askari and M. Tahani. Size-dependent dynamic pull-in analysis of beam-type MEMS under mechanical shock based on the modified couple stress theory. *Applied Mathematical Modelling*, 39(2):934–946, 2015. doi: 10.1016/j.apm.2014.07.019.

[14] W.-Y. Jung, W.-T. Park, and S.-C. Han. Bending and vibration analysis of S-FGM microplates embedded in Pasternak elastic medium using the modified couple stress theory. *International Journal of Mechanical Sciences*, 87:150–162, 2014. doi: 10.1016/j.ijmecsci.2014.05.025.

[15] A. Babaei, A. Ghanbari, and F. Vakili-Tahami. Size-dependent behavior of functionally graded micro-beams, based on the modified couple stress theory. *International Journal of Engineering and Technology Sciences*, 3(5):364–372, 2015.

[16] N. Shafiei, A. Mousavi, and M. Ghadiri. Vibration behavior of a rotating non-uniform FG microbeam based on the modified couple stress theory and GDQEM. *Composite Structures*, 149:157–169, 2016. doi: 10.1016/j.compstruct.2016.04.024.

[17] R. Aghazadeh, E. Cigeroglu, and S. Dag. Static and free vibration analyses of small-scale functionally graded beams possessing a variable length scale parameter using different beam theories. *European Journal of Mechanics – A/Solids*, 46:1–11, 2014. doi: 10.1016/j.euromechsol.2014.01.002.

[18] M. Fathalilou, M. Sadeghi, and G. Rezazadeh. Micro-inertia effects on the dynamic characteristics of micro-beams considering the couple stress theory. *Mechanics Research Communications*, 60:74–80, 2014. doi: 10.1016/j.mechrescom.2014.06.003.

[19] R. Ansari, R. Gholami, M.F. Shojaei, V. Mohammadi, and S. Sahmani. Bending, buckling and free vibration analysis of size-dependent functionally graded circular/annular microplates based on the modified strain gradient elasticity theory. *European Journal of Mechanics – A/Solids*, 49:251–267, 2015. doi: 10.1016/j.euromechsol.2014.07.014.

[20] M.A. Eltaher, S.A. Emam, and F.F. Mahmoud. Free vibration analysis of functionally graded size-dependent nanobeams. *Applied Mathematics and Computation*, 218(14):7406–7420, 2012. doi: 10.1016/j.amc.2011.12.090.

[21] F. Ebrahimi and E. Salari. Thermal buckling and free vibration analysis of size dependent Timoshenko FG nanobeams in thermal environments. *Composite Structures*, 128:363–380, 2015. doi: 10.1016/j.compstruct.2015.03.023.

[22] F. Ebrahimi and E. Salari. Nonlocal thermo-mechanical vibration analysis of functionally graded nanobeams in thermal environment. *Acta Astronautica*, 113:29–50, 2015. doi: 10.1016/j.actaastro.2015.03.031.

[23] A. Babaei and I. Ahmadi. Dynamic vibration characteristics of non-homogenous beam-model MEMS. *Journal of Multidisciplinary Engineering Science Technology*, 4(3):6807–6814, 2017.

[24] A. Babaei and C.X. Yang. Vibration analysis of rotating rods based on the nonlocal elasticity theory and coupled displacement field. *Microsystem Technologies*, 1–9, 2018. doi: 10.1007/s00542-018-4047-3.

[25] A. Babaei and A. Rahmani. On dynamic-vibration analysis of temperature-dependent Timoshenko micro-beam possessing mutable nonclassical length scale parameter. *Mechanics of Advanced Materials and Structures*, 2018. doi: 10.1080/15376494.2018.1516252.

[26] S. Azizi, B. Safaei, A.M. Fattahi, and M. Tekere. Nonlinear vibrational analysis of nanobeams embedded in an elastic medium including surface stress effects. *Advances in Materials Science and Engineering*, ID 318539, 2015. doi: 10.1155/2015/318539.

[27] B. Safaei and A.M. Fattahi. Free vibrational response of single-layered graphene sheets embedded in an elastic matrix using different nonlocal plate models. *Mechanics*, 23(5):678–687, 2017. doi: 10.5755/j01.mech.23.5.14883.

[28] A.M. Fattahi and B. Safaei. Buckling analysis of CNT-reinforced beams with arbitrary boundary conditions. *Microsystem Technologies*, 23:5079–5091, 2017. doi: 10.1007/s00542-017-3345-5

[29] A. Chakraborty, S. Gopalakrishnan, and J.N. Reddy. A new beam finite element for the analysis of functionally graded materials. *International Journal of Mechanical Sciences*, 45(3):519–539, 2003. doi: 10.1016/S0020-7403(03)00058-4.

[30] H.J. Xiang and J. Yang. Free and forced vibration of a laminated FGM Timoshenko beam of variable thickness under heat conduction. *Composites Part B: Engineering*, 39(2):292–303, 2008. doi: 10.1016/j.compositesb.2007.01.005.

[31] S. Pradhan and T. Murmu. Thermo-mechanical vibration of FGM sandwich beam under variable elastic foundations using differential quadrature method. *Journal of Sound and Vibration*, 321(1):342–362, 2009. doi: 10.1016/j.jsv.2008.09.018.

[32] A. Nateghi and M. Salamat-talab. Thermal effect on size dependent behavior of functionally graded microbeams based on modified couple stress theory. *Composite Structures*, 96:97–110, 2013. doi: 10.1016/j.compstruct.2012.08.048.

[33] A. Mahi, E.A. Bedia, A. Tounsi, and I. Mechab. An analytical method for temperature-dependent free vibration analysis of functionally graded beams with general boundary conditions. *Composite Structures*, 92(8):1877–1887, 2010. doi: 10.1016/j.compstruct.2010.01.010.

[34] A. Babaei, M.R.S. Noorani, and A. Ghanbari. Temperature-dependent free vibration analysis of functionally graded micro-beams based on the modified couple stress theory. *Microsystem Technologies*, 23(10):4599–4610, 2017. doi: 10.1007/s00542-017-3285-0.

[35] B. Safaei, R. Moradi-Dastjerdi, and F. Chu. Effect of thermal gradient load on thermo-elastic vibrational behavior of sandwich plates reinforced by carbon nanotube agglomerations. *Composite Structures*, 192:28–37, 2018. doi: 10.1016/j.compstruct.2018.02.022.

[36] J.N. Reddy. Nonlocal theories for bending, buckling and vibration of beams. *International Journal of Engineering Science*, 45(2-8):288–307, 2007. doi: 10.1016/j.ijengsci.2007.04.004.